Pharmaceutical Research, Vol. 24, No. 10, October 2007 (© 2007)
DOI: 10.1007/s11095-007-9304-6

Research Paper

Structural Development of Self Nano Emulsifying Drug Delivery Systems (SNEDDS) During *In Vitro* Lipid Digestion Monitored by Small-angle X-ray Scattering

Dimitrios G. Fatouros,[1,5] G. Roshan Deen,[2] Lise Arleth,[3] Bjorn Bergenstahl,[4] Flemming Seier Nielsen,[1] Jan Skov Pedersen,[2] and Anette Mullertz[1]

Received September 16, 2006; accepted March 22, 2007; published online April 26, 2007

Purpose. To investigate the structural development of the colloid phases generated during lipolysis of a lipid-based formulation in an *in vitro* lipolysis model, which simulates digestion in the small intestine.
Materials and Methods. Small-Angle X-Ray scattering (SAXS) coupled with the *in vitro* lipolysis model which accurately reproduces the solubilizing environment in the gastrointestinal tract and simulates gastrointestinal lipid digestion through the use of bile and pancreatic extracts. The combined method was used to follow the intermediate digestion products of a self nano emulsified drug delivery system (SNEDDS) under fasted conditions. SNEDDS is developed to facilitate the uptake of poorly soluble drugs.
Results. The data revealed that a lamellar phase forms immediately after initiation of lipolysis, whereas a hexagonal phase is formed after 60 min. The change of the relative amounts of these phases clearly demonstrates that lipolysis is a dynamic process. The formation of these phases is driven by the lipase which continuously hydrolyzes triglycerides from the oil-cores of the nanoemulsion droplets into mono- and diglycerides and fatty acids. We propose that this change of the over-all composition of the intestinal fluid with increased fraction of hydrolyzed nanoemulsion induces a change in the composition and effective critical packing parameter of the amphiphilic molecules, which determines the phase behavior of the system. Control experiments (only the digestion medium) or the surfactant (Cremophor RH 40) revealed the formation of a lamellar phase demonstrating that the hexagonal phase is due to the hydrolysis of the SNEDDS formulation.
Conclusions. The current results demonstrate that SAXS measurements combined with the *in vitro* dynamic lipolysis model may be used to elucidate the processes encountered during the digestion of lipid-based formulations of poorly soluble drugs for oral drug delivery. Thus the combined methods may act as an efficient screening tool.

KEY WORDS: Cryo-TEM; *in vitro* digestion; liquid crystals; nano-emulsions; oral delivery; SAXS.

INTRODUCTION

Oral administration is the most popular route of administration for the majority of drugs. However, poorly soluble drugs often have a low and variable oral bioavailability due to inherent low solubility and slow dissolution rate in the primarily aqueous contents of the gastrointestinal tract. In an attempt to improve the solubility-limited bioavailability associated with these compounds, the use of lipid-based formulations, in which the compounds can be in solution prior to oral administration, has attracted a lot of attention (1). However, the overall performance of these formulations is highly dependent on the intermediate phases produced during lipid digestion and their morphologies (2,3).

Therefore an *in vitro* method has been developed describing the behaviour of poorly soluble compounds under conditions simulating the fluids in the gastrointestinal tract. The method make it possible to explore the relation between the *in vitro* findings and the *in vivo* performance of the formulations (4). The *in vitro* dynamic lipid digestion model can offer information regarding drug partitioning during hydrolysis of triacylglycerides and help predicting which type of lipid will increase concentration of solubilized drug in the intestinal fluids (5–7). The model allows sampling at different

[1] Department of Pharmaceutics and Analytical Chemistry, The Danish University of Pharmaceutical Sciences, Universitetsparken 2, 2100, Copenhagen, Denmark.
[2] Department of Chemistry and iNANO Interdisciplinary Nano Science Center, University of Aarhus, Langelandsgade 140, 8000, Aarhus C, Denmark.
[3] Biophysics, Department of Natural Sciences, The Royal Veterinary and Agricultural University, Thorvaldensevej 40, 1871, Frederiksberg C, Denmark.
[4] Department of Food Technology, Center for Chemistry and Chemical Engineering, Lund University, P.O. Box 124, 22100, Lund, Sweden.
[5] To whom correspondence should be addressed. (e-mail: df@dfuni.dk)

time points offering the opportunity to follow the lipolytic process as a function of time.

The physicochemical nature of the lipid material in the GI tract was first described in the early 1960s (8,9). The liquid crystalline phase produced during lipid digestion was first confirmed by light microscopy (10,11). However, *in vivo* lipolysis is a dynamic process. Multilamellar liquid-crystalline phases are formed continuously at the surface of the oil droplets and have a high ratio of lipolytic products to bile salts (LP: BS ratio). They are transformed first to multilamellar vesicles and secondly to unilamellar vesicles by increasing incorporation of BS. By further incorporation of BS, the LP: BS ratio decreases to unity or lower, whereby unilamellar vesicles are transformed to mixed micelles (12).

The aim of the present study is to evaluate the use of Small-Angle X-ray Scattering coupled with the *in vitro* digestion model to elucidate the mechanisms occurring during digestion of lipid-based formulations. For this purpose a self nano-emulsifying drug delivery system is "digested" in conditions mimicking the fasted state in the gastrointestinal tract. Previously, SAXS has been used to investigate the effect of a microbial lipase on the formation of lipid liquid crystalline phases in a monoolein-water system (13,14). This study is to our best knowledge the first application of the method to investigate the dynamic process of digestion of pharmaceutical relevant lipid-based formulations.

MATERIALS AND METHODS

Materials

Pancreatin (porcine), bile extract (porcine) and sesame oil were purchased from Sigma-Aldrich, USA. 4-bromobenzeneboronic acid (BBBA) was purchased from Lancaster, Germany. Cremophor RH 40 was purchased from BASF, Germany and Maisine 35-1 from Gattefossé, France respectively. Phosphatidylcholine Epikuron 200 (purity, minimum 92%) was kindly donated from Degussa, Germany. The water used was obtained from a Milli-Q-water purification system, Millipore, MA, USA. All other chemicals were of analytical grade.

Preparation of Formulation for the Self-Nano Emulsifying Drug Delivery System (SNEDDS-formulation)

A previously developed self-nano emulsifying drug delivery system (SNEDDS) was used in this study (15). The SNEDDS formulation basically consists of a mixture of oil, surfactant and ethanol. When the formulation is dispersed in an aqueous phase, nano-sized surfactant-covered oil-droplets are spontaneously formed. The applied SNEDDS formulation consisted of a total of 60% w/w oil which was a mixture of long chain triglycerides (LCT): Sesame oil (30% w/w), containing mono-, di- and triacylglycerides (primarily oleic an linoleic), and Maisine 35-1 (30% w/w) mainly mono-, and diacylglycerides (primarily containing oleic and linoleic fatty acids), the surfactant Cremophor RH 40 (30% w/w) which is a polyethoxylated hydrogenated castor oil with a high HLB (12–14) and ethanol (10% w/w) which acts as a co-solvent.

Lipolysis Medium

In the current study a concentration of 5 mM of bile salts and 1 mM of phosphatidylcholine EPIKURON 200 (phospholipid fraction, min. 92% PC) (Degussa, Germany) was used. This simulates the fasted conditions in the GI tract (16). The phase equilibrium between Epikuron 200 and water has been characterized previously (17). The composition of the digestion buffer was 150 mM NaCl, 2 mM Trizma maleate pH 6.5 and the final volume 300 ml. The Trizma-maleate concentration was chosen to be low (2 mM) to secure that ionized fatty acids are able to change pH (18). A buffer with low capacity was chosen in order for the released fatty acids to be able to reduce the pH, thereby triggering the addition of NaOH. We chose pH 6.5 as a compromise between the optimum for the pancreas lipase, which is between 6 and 10 (19) and the measured small intestine pH, which is around 6.0–7.0 (20).

Preparation of Lipase Suspension

The lipase suspension was prepared in accordance with the method described previously (5) to give an activity of 800 USP units/ml. Briefly 16.6 g of pancreatin was weighted accurately, suspended in 110 ml of Millipore water at 37°C and mixed thoroughly. The suspension was centrifuged for 7 min at 4,000 rpm at 37°C and the pH of the supernatant was adjusted to 6.5 using 1.00 M NaOH. One hundred milliliters of the pH-adjusted supernatant was used for the study. In order to minimize denaturation, the time spent on preparing the suspension did not exceed 15 min. The lipase activity of pancreatin was determined in accordance with United States Pharmacopeia 26, 2003 (21).

In vitro Digestion Study

The experimental set-up of the *in vitro* lipolysis model is presented in Fig. 1. A pH-stat titrate a controlled volume of NaOH to maintain the initial pH. The number of OH^- ions

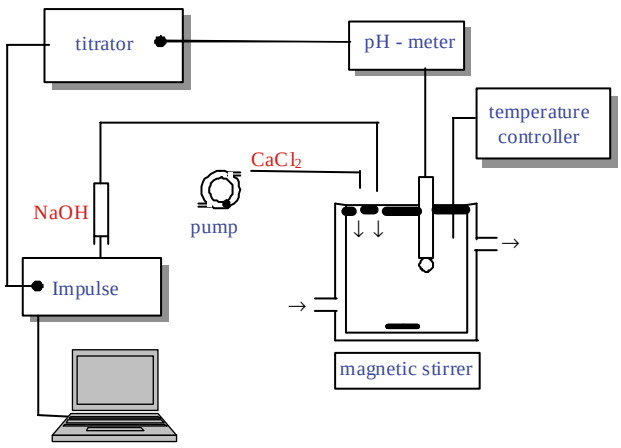

Fig. 1. Lipolysis set-up. It consists of a thermostated double wall reaction vessel, the pH-stat with the auto burette for the addition of NaOH, a peristaltic pump for the addition of $CaCl_2$ and the computer with the software for the titration experiments. The temperature is monitored during the experiment with a thermocouple. The experiment is performed under continuous agitation at 37°C.

present in the volume of the titrant can be equated with the fatty acid liberation caused by lipolysis.

The bile salt, phospatidylcholine and buffer of the lipolysis medium were mixed in a thermostatically controlled vessel (37°C). Three g of the SNEDDS formulation was added to the obtained 300 ml of the bile salt medium, giving a final concentration of 1% w/v. The pH of the medium was adjusted to 6.5 with 1.0 M NaOH. The lipolysis process was initiated by adding the 100 ml lipase suspension. In the dynamic lipolysis model the continuous addition of calcium chloride solution serves to control accumulation of FA in the medium by forming insoluble calcium FA soaps, which precipitate thus removing FA from the system and preventing accumulation (22). Therefore a continuous addition of a 0.5 M Ca^{2+} solution was started at time zero with a dispensing rate of 0.045 mM/min. Throughout the study pH was kept constant at 6.5 by means of a pH-stat (Titrino 718 with burette from Methrohm, Switzerland). The software used was Tinet, version 2.3 also from Methrohm.

At 0, 5 15, 30, 60 and 90 min, 20-ml samples were withdrawn and the lipase was inhibited immediately with a 4-bromobenzeneboronic acid (BBBA) Lancaster, Germany solution as described previously (5). The time zero sample was taken just after adjustment of the pH in the medium.

Lipolysis studies containing only the digestion medium or Cremophor RH 40 in the same amount as present in the SNEDDS formulation were performed as well, serving as controls.

Small Angle X-ray Scattering Studies

The samples withdrawn at 0, 5 15, 30, 60 and 90 min were transferred to quartz capillaries and SAXS measurements were performed at 37°C on a Bruker Nanostar SAXS instrument optimized for solution scattering (23). Approximately 0.3 ml of sample was used for each measurement. The duration between the sample quenching and the SAXS pattern acquisition was approximately 10 h. In order to investigate the stability of the samples with respect to phase separation and sedimentation, SAXS measurements on the same samples were performed several times with waiting periods in between. Data collected from the scattering patterns were converted to intensity *vs* the scattering vector $q = (4\ \pi/\lambda\ )\ \sin\ (\theta)$, where $\lambda = 0.154$ nm is the X-ray wavelength and 2θ is the angle between the incident and scattered X-rays.

Cryo-TEM Studies

The samples for the Cryo-TEM studies were prepared in a controlled environment vitrification system (CEVS). A small amount of the sample (5 μl) was put on a carbon film supported by a copper grid and blotted with filter paper to obtain a thin liquid film on the grid. The grid was quenched in liquid ethane at −180°C and transferred to liquid nitrogen (−196°C). The oil droplets in Trizma pH 6.5 were visualized with Cryogenic electron microscopy, carried out with a TEM microscope (Philips CM120 BioTWIN Cryo) equipped with a post column energy filter (GATAN GIF 100) using an Oxford CT3500 cryoholder. The acceleration voltage was 120 kV and the working temperature, −180°C. The images were recorded with a CCD camera (Gatan 791) under low dose conditions. The defocus was approximately 1 μm.

RESULTS

Size Distribution of the Nanoemulsion Droplets Formed by the SNEDDS Formulation

The Cryo-TEM analysis shows that spherical emulsion droplets are formed upon dilution of the SNEDDS emulsion in Trizma maleate buffer, pH 6.5 [1% w/v] (Fig. 2a). The SNEDDS size distribution was determined by Image Analysis program (24) (Fig. 2b). The average diameter of the oil droplets obtained this way was 33.7 ± 8.4 nm. These values were in good agreement with the average size of the oil-cores of the droplets of $\overline{D} = 37.8$ nm as determined from the SAXS data by the fitting of a structural model for polydisperse spherical oil-droplets surrounded by a lipid/surfactant layer (25) (Fig. 2c). The SAXS analysis furthermore showed that the surrounding lipid/surfactant layer has a thickness of on average 2.5 nm and that the obtained droplet size distribution has a standard deviation, σ, of 6.7 nm, corresponding to $\sigma/\overline{D} = 18\%$ (Fig. 2d).

Lipolysis of SNEDDS Formulation

The consumption of NaOH during the study, reflecting the progress of lipolysis, is depicted in Fig. 3. Generally when triacylglycerides hydrolyze, one monoglyceride and two fatty acids are formed, and the consumption of NaOH can be directly related to the fatty acids formed during lipolysis. The percentage of hydrolyzed triacylglycerides was calculated from the consumption of NaOH or in other words the number of OH^- ions in the titrant.

Studies with only the digestion medium and the surfactant Cremophor RH 40 were performed as well serving as controls. As can be seen from Fig. 3, Cremophor RH 40 is not hydrolyzed, on the contrary, inhibits the lipolysis process (the consumption of NaOH is reduced in the presence of the surfactant, compared with the lipolysis only containing the digestion medium). However at the end of the experiment (after 90 min) the values are comparable.

The consumption of NaOH during the lipolysis of the SNEDDS formulations differs significantly. This could be attributed to the fact that the starting materials were from different batches.

SAXS Analysis

The SAXS data recorded during the digestion process of the SNEDDS formulation in fasted conditions are shown in Fig. 4. Generally the relation between the Bragg distances for a sample corresponds to the symmetries of liquid crystalline phases formed. These distances follow the relation 1, √4, √9 for lamellar phases and the relation 1, √3, √4 for hexagonal phases.

As it was expected, at the beginning of the reaction (0 mins) the scattering intensity for both samples showed no signs of liquid crystalline phases (Fig. 4a). After 5 min when approximately 26% of the formulation (first experiment) had

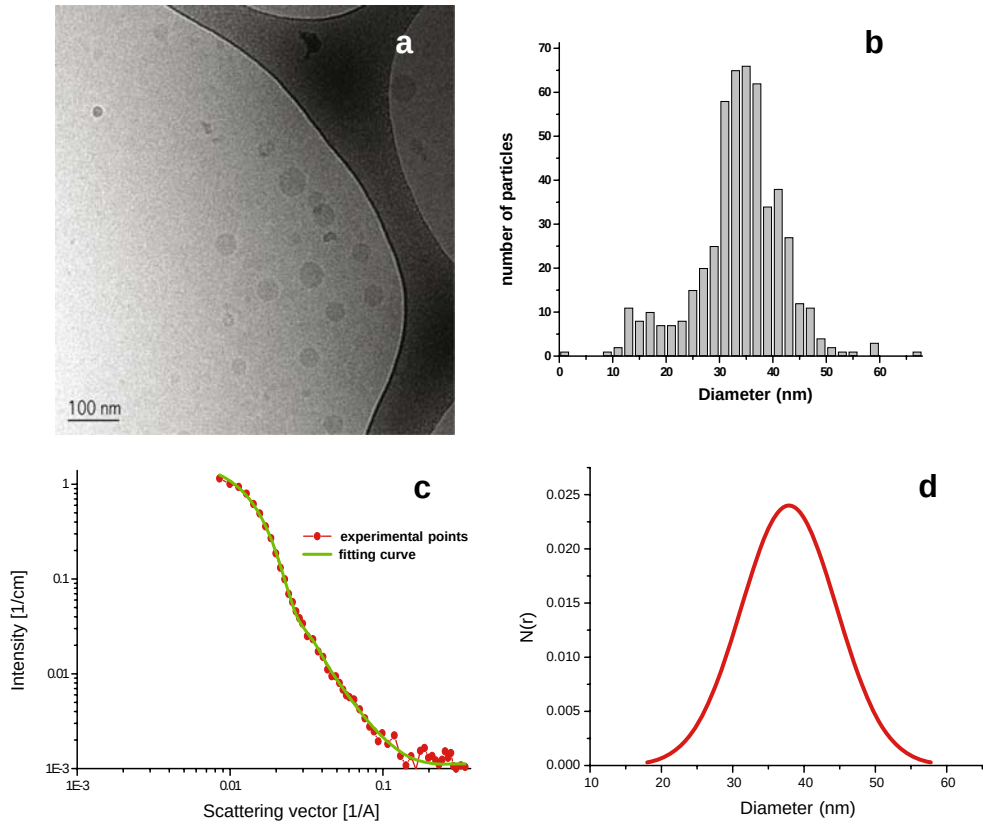

Fig. 2. a. Cryo-TEM image of SNEDDS dispersed in 2 mM Trizma buffer pH 6.5 giving a final concentration of 1% w/v. **b**. Size distribution of SNEDDS in Trizma buffer pH 6.5. **c**. SAXS data of SNEDDS dispersed in 2 mM Trizma buffer pH 6.5 with a final concentration of 1% w/v. Experimental points and fit results of the polydisperse core-shell model for the droplets. **d**. Droplets size distribution, *N(r)*, obtained from the SAXS model fits

been hydrolyzed, a Bragg-like peak appeared at $q = 1.3$ nm^{-1} corresponding to a Bragg spacing $d = 4.8$ nm (Fig. 4b, black line). After 5 min of hydrolysis in the second experiment only 18% of the formulation had been hydrolyzed, and no Bragg peaks could be seen, indicating that the appearance of the Bragg peaks are dependent on the degree of hydrolysis (Fig. 5b, red line).

After, 15 min an additional, but much smaller peak, became visible at $q = 4.0$ nm^{-1} corresponding to a Bragg spacing of $d = 1.6$ nm. This scattering picture persisted up to 30 min (Fig. 4c and d, black line) corresponding to 60% of hydrolysis of the formulation (first experiment). A similar scattering picture appears for the second experiment as well, when 35% of the lipid material was hydrolyzed, with the appearance of a small peak visible at $q = 1.3$ nm^{-1} corresponding to a Bragg spacing $d = 4.8$ nm (Fig. 4c, red line) followed by the appearance of three Bragg like peaks at $q = 1.3$ nm^{-1} corresponding to a Bragg spacing $d = 4.8$ nm, at $q = 2.6$ nm^{-1} corresponding to a Bragg spacing of $d = 2.4$ nm and at $q = 4.0$ nm^{-1} corresponding to a Bragg spacing of $d = 1.6$ nm (Fig. 4d, red line).

After 60 min, when the hydrolysis had reached 86% for the first experiment, an additional peak appeared at $q = 1.9$ nm^{-1} corresponding to a Bragg spacing of $d = 3.3$ nm (Fig. 4e, black line). However in the second experiment only 40% of lipolysis had been obtained after 60 min and therefore only the lamellar phase was present (Fig. 4e, red line). This could be due to the lower hydrolysis values obtained for the second one.

The intensity of the peak grew strongly (Fig. 4e and f, black line) and at the end of the process (100% of hydrolysis), a fourth peak became visible at $q = 3.3$ nm^{-1} corresponding to Bragg spacings of $d = 1.9$ nm (Fig. 4f, black line) for the first

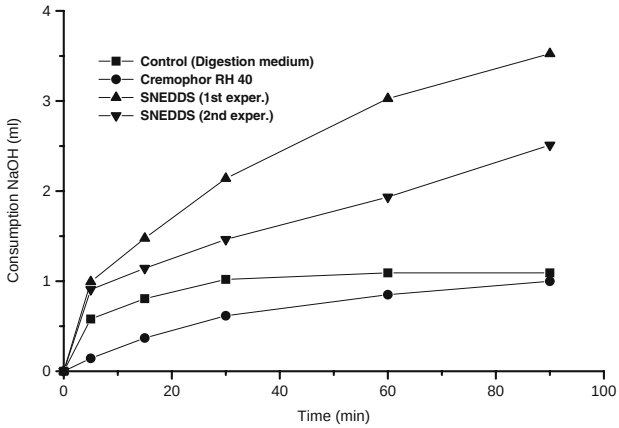

Fig. 3. Consumption of NaOH (ml) during hydrolysis of the control (only the digestion medium) (n = 1), the surfactant (Cremophor RH 40) (n = 1) and the SNEDDS formulations (n = 2).

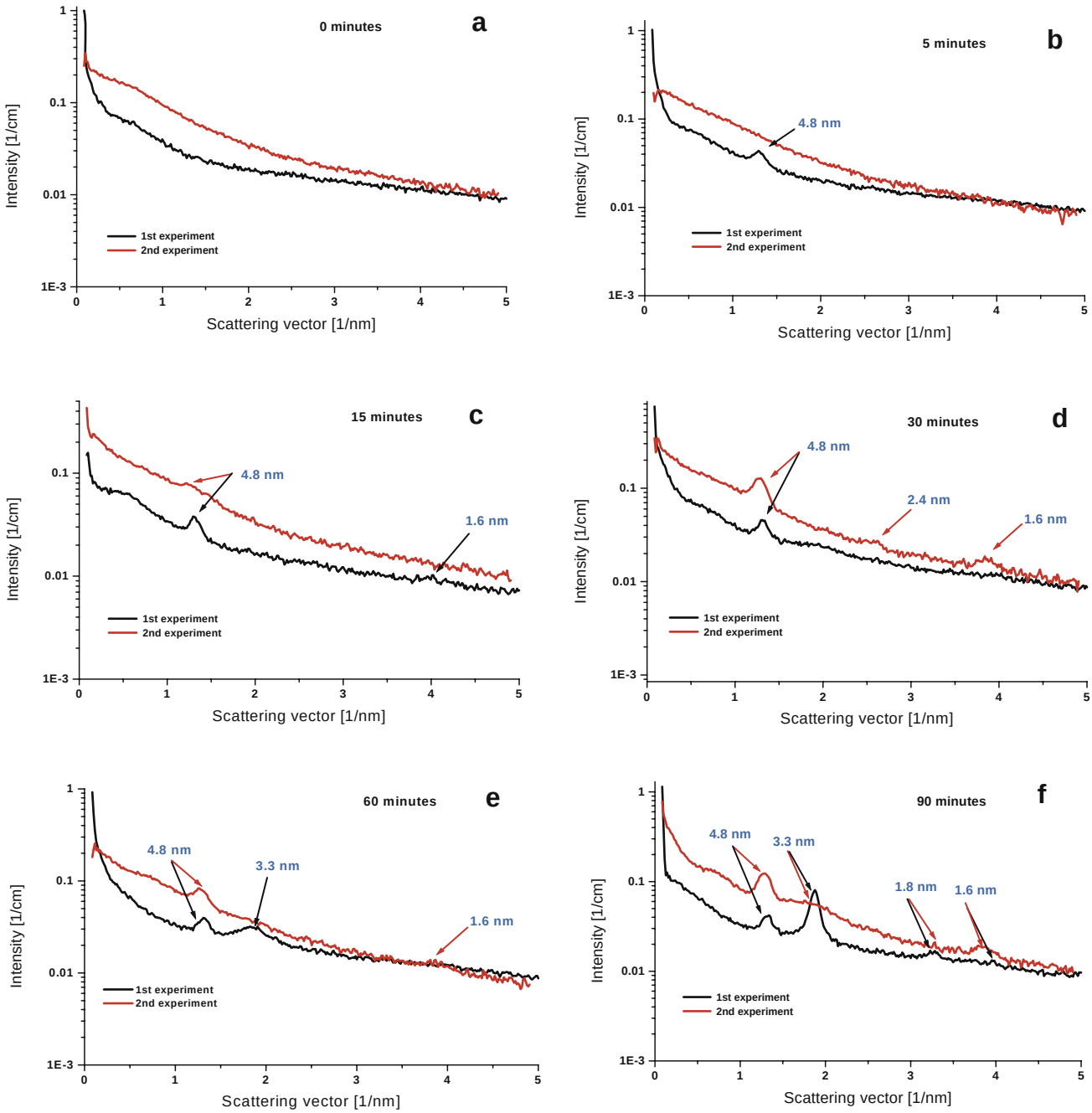

Fig. 4. SAXS spectra recorded for the SNEDDS formulation during digestion at 0, 5, 15, 30, 60 and 90 min. The intensity is plotted versus the wave vector. For the peaks $q = 2\pi/d$, where d is the spacing between the lattice planes. The sequence of phase development is the following (first experiment): **a**. no phases (0 min), **b**. Lamellar phase (5 min), **c**. Lamellar phase (15 min) **d**. Lamellar phase (30 min), **e**. Lamellar and Hexagonal phase (60 min), **f**. Lamellar and Hexagonal phase (90 min). Second experiment **a**. no phases (0 min), **b**. no phases (5 min), **c**. Lamellar phase (15 min) **d**. Lamellar phase (30 min), **e**. Lamellar phase (60 min), **f**. Lamellar and Hexagonal phase (90 min).

experiment. For the second one the same peaks appear but with weaker peak intensities probably due to the lower degree of lipolysis. The samples were found stable since three repeated SAXS measurements showed that phase separation and sedimentation did not occur during the analysis (data not shown).

As explained, the peaks appeared in pairs, first the peaks at peaks at 1.3 and 4.0 nm^{-1} and then the peaks at peaks at 1.9 and 3.3 nm^{-1}. Our data are in agreement with the formation of an initial lamellar phase, (peaks at 1.3 and 4.0 nm^{-1}) followed by the formation of a hexagonal phase (peaks at 1.9 and 3.3 nm^{-1}) during the digestion process. A lamellar phase gives the characteristic ratio 1:2:3:4:... in peak position. We only observe the first and third order peaks at the first experiment of the SNEDDS formulation. This is probably due to extinction of the second order peak due to form factor oscillations of the lamellar structure (26,27). The hexagonal phase gives the characteristic peak position pattern as 1: √3

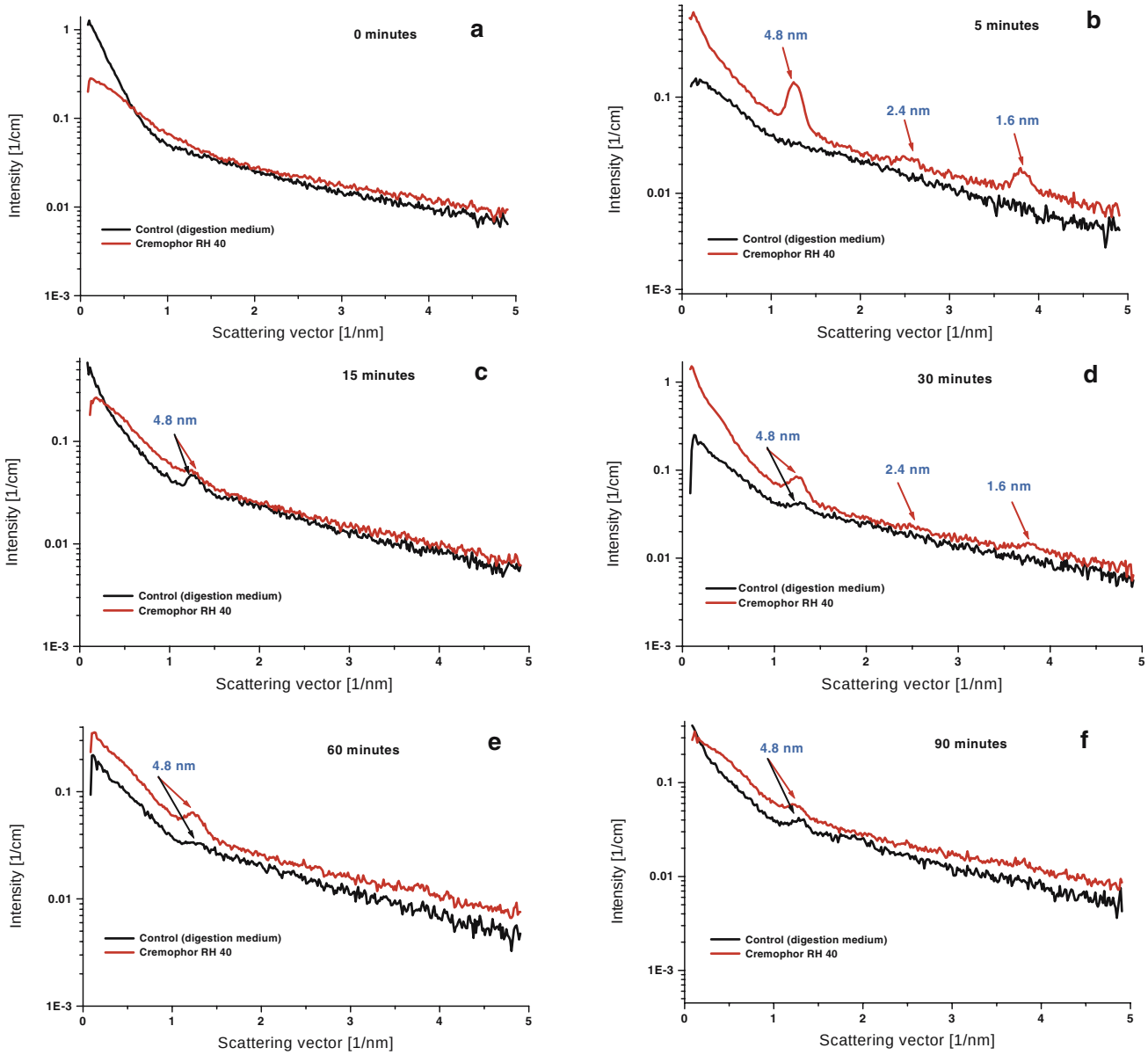

Fig. 5. SAXS spectra recorded for the control (only the medium) and the Cremophor RH 40 during digestion at 0, 5, 15, 30, 60 and 90 min. The intensity is plotted versus the wave vector. For the peaks $q = 2\pi/d$, where d is the spacing between the lattice planes. The sequence of phase development for the control is the following: **a**. no phases (0 min), **b**. no phases (5 min), **c**. Possible lamellar phase (15 min) **d**. possible lamellar phase (30 min), **e**. possible lamellar phase (60 min), **f**. possible lamellar phase (90 min) and for the Cremophor RH 40 : **a**. no phases (0 min), **b**. Lamellar phase (5 min), **c**. Lamellar phase (15 min) **d**. Lamellar phase (30 min), **e**. Lamellar phase (60 min), **f**. Lamellar phase (90 min).

corresponding to $(h, k) = (1, 0), (1, 1)$. Furthermore the gradual change of the SAXS data and Bragg peak intensities with time show that the amount of each phase is changing with time, and thus that the lipolysis of lipid-based formulations is a dynamic process. Indeed, the lamellar phase is dominating up to 60% of hydrolysis of the formulation, however, as the lipolysis proceeds a hexagonal phase appears co-existing with the lamellar phase up to 80% of hydrolysis, and at the end, when the lipolysis has been completed, the hexagonal phase becomes the dominating phase in the system.

In order to elucidate how the formation of the intermediate colloidal phases can be affected by the presence of the digestion medium (alone) and Cremophor RH 40 were digested and their SAXS spectra were recorded under the same conditions as the SNEDDS formulation.

The SAXS data recorded for the control (digestion medium) and the Cremophor RH 40 are illustrated in Fig. 5. The scattering intensity for the control exhibited no signs of liquid crystalline phases up to 15 min. After 15 min, a Bragg-like peak appeared at $q = 1.3\ \text{nm}^{-1}$ corresponding to a Bragg spacing $d = 4.8$ nm (Fig. 5c, black line). This scattering picture persisted up to 90 min (Fig. 5d, e and f, black line). However with one peak reflection it is not possible to assign any structures.

In the case of Cremophor RH 40, as it was expected, at the beginning of the reaction (0 min) the scattering intensity exhibited no signs of liquid crystalline phases (Fig. 5a). After 5 min of lipolysis, three Bragg-like peaks appeared at $q = 1.3$ nm^{-1} corresponding to a Bragg spacing $d = 4.8$ nm, at $q = 2.6$ nm^{-1} corresponding to a Bragg peak at $d = 2.4$ nm and at $q = 4.0$ nm^{-1} corresponding to a Bragg spacing of $d = 1.6$ nm giving evidence to the formation of a lamellar phase (1:2:3...), (peaks at 1.3, 2.6 and 4.0 nm^{-1}) during the digestion process (Fig. 5b, red line). This phase persisted up to 90 min (Fig.c, d, e and f, red line)

Since the intensities of the peaks corresponding to this phase are practically constant, at least for the studied time points, we can also conclude that it persists. Furthermore 60% of hydrolysis of the formulation could be considered as the "ceiling" for the formation of lamellar phases based on the peak intensities since beyond the 60% hydrolysis point and up to the end of the process only small changes are observed (Fig. 5). However, this phenomenon is rather system specific since the hydrolysis rate is highly depending on the components of the formulation.

DISCUSSION

The fact that the formation of lamellar phases during lipid digestion is a very quick process has also been shown previously by light microscopy studies, in which the lamellar structures formed already 1.5 min after the initiation of the reaction (10). In contrast, the development of the hexagonal phase is a rather slow procedure. Consequently the following question arises: What are the mechanism and the origin of these two phases?

The proposed mechanism for the lipolysis of e.g. oil droplets in the intestine describes the accumulation of different kinds of polar lipids on the surface of the oil droplet as a result of the hydrolysis via the interfacial action of pancreatic lipase. This lipid material (mainly monoglycerides and fatty acids) produces multilamellar liquid crystalline phases on the surface of the droplets which, due to the interaction with the surface active bile salt, are gradually "detached" from the surface and produce multilamellar vesicles which undergo a transformation initially to first unilamellar vesicles and later to mixed micelles upon the bile salt interaction (12,28). Upon their formation on the surface of the oil droplets there are two ways for the lipid material to be removed from the surface: Either via the formation of calcium soaps or by being solubilized in mixed bile salt micelles. These multilamellar phases have been visualized with freeze fracture electron microscopy as rough surfaces with variable distance between the lamellae (12). However the exact structure of these phases has not been fully clarified and it was not clear whether or not these multilamellar phases possessed a cubic structure (12). Previously, a possible transitory hexagonal phase was also observed during lipolysis of an emulsion with pancreatic lipase in the absence of bile salts (29).

In the current study the situation is slightly different as the initial oil droplets are rather small ($R \approx 40$ nm) as compared to those encountered in the above description. However, we confirm the appearance of a succession of liquid crystalline phases (lamellar phase followed by a hexagonal phase). Furthermore, the evolution of these phases appears to be directly related to the amount of the lipolytic products generated on the surface of the droplets. Before the lipolysis starts the samples do not contain any visible liquid crystallinity, but during the lipolysis process, first a lamellar and then a hexagonal phase appears. Thus we propose that a mechanism similar to the above described can account for the structural changes that take place in the SNEDDS system during its digestion.

The observed order of appearance of these two phases is in good agreement with that observed in typical phospholipid systems (30) where lamellar bilayer structures form at low concentrations of phospholipid in water, whereas at relatively higher phospholipid concentrations (or higher temperatures), the dehydration of the polar headgroups may induce the formation of an inverse hexagonal phase, sometimes by intermediate of an inverse cubic phase. The formation of these phases may generally be explained in terms of the molecular shape and the critical packing parameter, v/Al_c, of the amphiphilic molecules, where v is the partial specific molecular volume of the amphiphilic molecule, A, its area per headgroup at the hydrophobic–hydrophilic interface and l_c, the hydrocarbon chain length (31,32). For amphiphilic molecules with a critical packing parameter close to unity, a lamellar structure is favored. This is typically the case for highly hydrated phospholipids. Whereas critical packing parameters larger than unity favors the formation of inverted structures.

The formation of mono- and diglycerides and fatty acids by pancreatic lipase on the oil surface changes the overall composition of the amphiphilic layer and thereby change the average critical packing parameter of the amphiphilic molecules. In the beginning of the experiment, the amphiphilic phase is composed by a mixture of cremophor RH 40, phosphatidylcholine and bile salt. However, with the formation of the monoglycerides and fatty acids with their relatively small polar headgroups and long hydrocarbon chains (C_{18}-chains) the amphiphilic phase is changed in a more apolar direction and towards an, on average, increasing critical packing parameter. This explains the formation of first the lamellar structure and later the hexagonal structure, which is then, most likely, an inverted hexagonal (30–32).

While the general succession of the observed liquid crystalline morphologies can be rationalized in terms of the critical packing parameter theory, the detailed molecular composition of the different phases is more difficult to assess in the complex system studied. It is well documented in the literature that monoglycerides and fatty acids will generate liquid crystalline phases upon their dispersion in aqueous media (33,34). Thus, we expect that the observed phases contain significant amounts of the lipolysis products. Previous studies have shown that phosphatidylcholine molecules are able to partition in the interface of a triglyceride emulsion and the aqueous phase (35). Since the lipolysis medium contains phosphatidylcholine its hydrolysis product lysophosphatidylcholine may also be present in the liquid crystalline phases along with non-hydrolyzed phosphatidylcholine.

The values obtained in the current study for the lamellar phases give a Bragg spacing of 4.8 nm. Freeze fracture electron microscopy studies of an olive oil emulsion using

similar conditions of pure lipase/colipase with 4 mM cholate/taurocholate and 30 min of incubation in a similar manner revealed that the lamellae thickness was 5.7 ± 0.82 nm (12). This value is comparable to the lamellae thickness that we observe, though slightly higher, which may be explained by the relatively higher contents of the more extended mono-unsaturated oleic acid in olive oil as compared to the more linoleic acid rich sesame oil/maisine 35-1 oil composition used in the present study. In both cases the lamellae thickness is in good agreement with predictions based on the chain-length of the C18-chains of the fatty acids that have a maximal extension of approximately 24 Å (36). This leads to a bilayer thickness close to 5 nm in dry/water-poor phases. Larger lamellar repeat distances can be obtained if an aqueous layer can be stabilized between the bilayer films.

In a model system containing mixtures of bile salts, cholesterol and mixed intestinal lipids [myristic acid, monomyristoylglycerol, dimyristoylphosphatidylcholine, 5:1:1] with a total lipid amount of 8% w/v after equilibration for 7 days at room temperature two lamellar reflections with Bragg spacings of 8.2 and 4.1 nm were recorded with SAXS (37). However these studies were performed after equilibrium which is not the case in the current study and the total lipid amount used was rather high compared with the more physiological levels where other studies have been conducted (1%) (38). High amounts of lipids in such model mixtures induce the formation of multilamellar vesicles as has been shown previously (38).

Additional SAXS studies of fatty acids with potassium soaps (1:1) after equilibrium at 20°C revealed the formation of lamellar and hexagonal liquid crystals depending on the level of hydration (39). In the case of potassium hydrogen dioleate soap at 40% of water 3 orders of hexagonal reflections, in a ratio 1:√3: √4, were observed with a first peak of 5.47 nm. Between 50 and 80% of water hexagonal and lamellar phases co-exist and finally at 90% of water, two lamellar reflections were observed (39). Again in good agreement with theory (31,32) and in accordance with the general findings in phospholipid systems (30).

The fact that calcium is also present in our system could eventually lead to the formation of calcium soaps. However in contrast with other approaches where the calcium chloride is pre-added at the beginning of the reaction (10,12), we have, in the current study, added the calcium chloride constantly during the hydrolysis of the formulation. In this manner the calcium soap formation may be a slower process since at the beginning of the reaction only small amounts of calcium are present in the system.

The second phase observed after 60 min corresponding to more than 90% of hydrolysis of the nanoemulsion gives evidence of a hexagonal phase with a lattice distance of 3.3 nm. Generally monoglycerides can induce the formation of hexagonal phases (33,34). In a system formed by monoolein and oleic acid buffered to pH 6.5, an increase of the oleic acid/monoolein ratio, keeping the total lipid constant to 1% w/v, resulted in a transfer from cubic to a reversed hexagonal phase (40). However an unknown viscous isotropic phase was recognized between the hexagonal and an L2 phase. At this area the ratio between MG: FA was approximately 1:2 which is close to the amount of the lipolytic produced theoretically during the hydrolysis of triacylglycerols. In the same study, a mixture of oleic acid/monoolein was dispersed in 10 mM NaTDC at pH 6.5 with 50 mM Tris-Maleate and 150 mM NaCl gave a picture similar to an L2 phase by X-ray diffraction. At a ternary phase diagram of oleic/sodium oleate/water at 38°C, sodium oleate form several different phases (crystalline-lamellar liquid crystalline-hexagonal liquid crystalline-micellar liquid) as the water content increases (41). Phase diagrams of monoglycerides/sodium taurocholate/water were characterized after equilibrium at 25°C with DLS and NMR (42). A hexagonal phase was identified between an isotropic micellar and liquid crystalline phases however the X-ray analysis could not give unequivocal evidence of this phase.

While the existence of the lamellar phases during lipid digestion is well documented in the literature either with studies using the *in vitro* digestion model (12,29) or by characterization of lipolytic products (37,38,40,42), evidence of hexagonal phase, has been rather alluded than recognized at least using the *in vitro* lipid digestion model. A possible transitory hexagonal phase was reported during lipid digestion of a trioleylglycerol emulsion with pancreatic lipase in the absence of bile salts at pH 8 visualized by freeze fracture electron microscopy (29). This is the first report demonstrating that hexagonal phases can be formed during lipid digestion in a dynamic environment.

The current results provide a strong indication that the appearance of the hexagonal phase is related with the hydrolysis of the SNEDDS which is a consequence of the composition of the formulation. Additionally our data demonstrated that despite the general sequence of the formation (lamellar phase, hexagonal phase) of the intermediate products the time of appearance of these phases is not identical for the same type of experiments indicating that this is highly dependent on the amount of the hydrolyzed material.

Furthermore the role of the surfactant to the formation of intermediate colloid phases was investigated. When comparing the SAXS spectra of the digestion medium and the Cremophor RH 40 it can be assumed that in both cases a lamellar phase is formed (Fig. 5). However what is the reason that only the first peak appears in the digestion medium (control) making difficult to assign any structures compared with the clear picture of a lamellar phase formed in the presence of Cremophor RH 40? Looking at the consumption profiles (Fig. 3) for the control and the surfactant it can be concluded that Cremophor RH 40 is not hydrolyzed and most important inhibits the rate of the hydrolysis at least at the beginning of the process.

Moreover based on the composition of these two media (control and surfactant) the main contributor for the formation of a lamellar phase is phosphatidylcholine. In the digestion medium only phosphatidylcholine can be hydrolyzed to lyso-phosphatidylcholine. Thus Cremophor RH 40 reduces the rate of hydrolysis, or in other words, inhibits the hydrolysis of phosphatidylcholine to lyso-phosphatidylcholine, allowing the formation of a lamellar phase in a more pronounced way compared with the digestion medium alone. This can be reflected with the appearances of three Bragg-like peaks in the system containing the surfactant, corresponding to a lamellar structure.

Several parameters like the level of the bile salts in the medium, the size (e.g. oil) or the composition (medium chain

triglycerides, surfactants) of the formulation, the different amount of calcium chloride or pancreatic lipase might have an impact to the formation of the intermediate lipolytic products; these are questions to be answered.

However the current study lays out the framework for future work since the lipid digestion of pharmaceutical interest formulations is studied in a dynamic, non-equilibrated environment mimicking the in vivo conditions.

CONCLUSIONS

In view of the previous findings it has been demonstrated that small-angle X-ray scattering analysis applied on the dynamic lipolysis model provides important information for the generated phases and their molecular architecture and might improve the understanding of the mechanism behind *in vivo* degradation of lipid-based formulations. Furthermore this is a new approach for studying the intermediate lipolytic products of lipid digestion offering important information, on the nano-scale phenomena taking place on the surface of the oil droplets, giving structural evidence of phases that other techniques are not able to offer because of their susceptibility to artifacts or resolution limitations. Identification and characterization of the intermediate lipolytic products formatted during lipid digestion could offer new insights for designing and optimizing new oral lipid-based formulations and possibilities for predicting their *in vivo* behavior.

ACKNOWLEDGEMENT

The Cryo microscopy has been performed at the Biomicroscopy unit at the Centre of Chemistry and Chemical Engineering at Lund University, Sweden. The authors are grateful to Mrs Gunnel Karlsson for the skilful assistance with the Cryo-TEM instrument. This work is financially supported from Drug Research Academy (DRA), The Danish University of Pharmaceutical Sciences. Phosphatidylcholine EPIKURON 200 was kindly donated from Degussa, Germany.

REFERENCES

1. C. W. Pouton. Lipid formulations for oral administration of drugs: non-emulsifying, self-emulsifying and 'self-micro-emulsifying' drug delivery systems. *Eur. J. Pharm. Sci.* **11**:S93–S98 (2000).
2. C. J. H. Porter, A. M. Kaukonen, A. Taillardat-Bertchinger, B. J. Boyd, J. M. O'Connor, G. A. Edwards, and W. N. Charman. Use of *in vitro* lipid digestion data to explain the in vivo performance of triglyceride-based oral lipid formulations of poorly water-soluble drugs: studies with halofantrine. *J. Pharm. Sci.* **93**:1110–1121 (2004).
3. G. A. Kossena, W. N. Charman, B. J. Boyd, and C. J. H. Porter. Influence of the intermediate digestion phases of common formulation lipids on the absorption of a poorly water-soluble drug. *J. Pharm. Sci.* **94**:481–492 (2005).
4. D. Fatouros, and A. Müllertz. Using *in vitro* dynamic lipolysis modelling as a tool for exploring IVIVC relationships for oral lipid-based formulations. In D. Hauss (ed.), *Lipid-based Formulations for Oral Drug Delivery*, Taylor & Francis, New York (in press).
5. N. H. Zangenberg, A. Müllertz, H. G. Kristensen, and L. Hovgaard. A dynamic *in vitro* lipolysis model. I. Controlling the rate of lipolysis by continuous addition of calcium. *Eur. J. Pharm. Sci.* **14**:115–122 (2001).
6. N. H. Zangenberg, A. Müllertz, H. G. Kristensen, and L. Hovgaard. A dynamic *in vitro* lipolysis model. II: evaluation of the model. *Eur. J. Pharm. Sci.* **14**:237–244 (2001).
7. J. O. Christensen, K. Schultz, B. Mollgaard, H. G. Kristensen, and A. Müllertz. Solubilisation of poorly water-soluble drugs during *in vitro* lipolysis of medium- and long-chain triacylglycerols. *Eur. J. Pharm. Sci.* **23**:287–296 (2004).
8. A. F. Hofmann and B. Borgstrom. Physico-chemical state of lipids in intestinal content during their digestion and absorption. *Fed. Proc.* **21**:43–50 (1962).
9. A. F. Hofmann and B. Borgstrom. Intraluminal phase of fat digestion in man-lipid content of micellar + oil phases of intestinal content obtained during fat digestion + absorption. *J. Clin. Invest.* **43**:247–257 (1964).
10. J. S. Patton and M. V. Carey. Watching fat digestion. *Science* **204**:145–148 (1979).
11. J. S. Patton, R. D. Vetter, M. Hamosh, B. Borgstrom, M. Lindstrom, and M. C. Carey. The light-microscopy of triglyceride digestion. *Food Microstruc.* **4**:29–41 (1985).
12. M. W. Rigler, R. E. Honkanen, and J. S. Patton. Visualization by freeze fracture, *in vitro* and in vivo, of the products of fat digestion. *J. Lipid Res.* **8**:836–857 (1986).
13. J. Borne, T. Nylander, and A. Khan. Effect of lipase on different lipid liquid crystalline phases formed by oleic acid based acylglycerols in aqueous systems. *Langmuir* **18**:8972–8981 (2002).
14. F. Caboi, J. Borne, T. Nylander, A. Khan, A. Svedsen, and S. Patkar. Lipase action on a monoolein/sodium oleate aqueous cubic liquid crystalline phase—a NMR and X-ray diffraction study. *Colloids Surfac. B-Bionter.* **26**:159–171 (2002).
15. F. S. Nielsen, E. Gibault, H. Ljusberg-Wahren, L. Arleth, J. S. Pedersen, and A. Müllertz. Characterization of prototype self-nano emulsifying formulations of lipophilic compounds. *J. Pharm. Sci.* **96**:876–892 (2007).
16. B. L. Pedersen, H. Brondsted, H. Lennernas, F. N. Christensen, A. Müllertz, and H. G. Kristensen. Dissolution of hydrocortisone in human and simulated intestinal fluids. *Pharm. Res.* **2**:183–189 (2000).
17. B. Bergenstahl and K. Fontell. Phase equilibria in the system soyabean lecithin water. *Prog. Coll. Pol. Sci.* **68**:48–52 (1986).
18. J. P. Reymond and H. Sucker. *In vitro* model for cyclosporine intestinal absorption in lipid vehicles. *Pharm. Res.* **5**:673–676 (1988).
19. Y. Gargouri, H. Moreau, and R. Verger. Gastric lipases: biochemical and physiological studies. *Biochim. Biophys. Acta* **1006**:255–271 (1989).
20. J. B. Dressman, R. R. Berardi, C. L. Dermentzoglou, T. L. Russell, S. P. Schmaltz, J. L. Barnett, and K. M. Jarvenpaa. Upper gastrointestinal (GI) pH in young, healthy men and women. *Pharm. Res.* **7**:756–761 (1990).
21. The United States Pharmacopoeia/The National Formulary, (USP 26/NF21). United States Pharmacopeia Convection, Inc., Rockville USP 26, 2003.
22. K. J. MacGregor, J. K. Embleton, J. E. Lacy, A. E. Perry, L. J. Solomon, H. Seager, and C. W. Pouton. Influence of lipolysis on drug absorption from the gastro-intestinal tract. *Adv. Drug Deliv. Rev.* **25**:33–46 (1997).
23. J. S. Pedersen. A flux- and background-optimized version of the NanoSTAR small-angle X-ray scattering camera for solution scattering. *J. Appl. Crystall.* **37**:369–380 (2004).
24. D. Wilcox, B. Dove, D. McDavid, and D. Greer. UTHSCSA Image Tool for Windows Vision 3. The University of Texas Health Science Center in San Antonio USA, 2002.
25. J. S. Pedersen. Modelling of small-angle scattering data from colloids and polymer systems. In P. Lindner, and Th. Zemb (eds.), *Neutrons, X-rays and Light: Scattering Methods Applied to Soft Condensed Matter*, Elsevier, Dordrecht, 2002, pp. 73–102.
26. K. Fontel. Structure of lamellar liquid crystalline phase in aerosol-OT water system. *J. Coll. Int. Sci.* **44**:318–329 (1973).
27. G. Pabst, M. Rappolt, H. Amenitsch, and P. Laggner. Structural information from multilamellar liposomes at full hydration: full q-range fitting with high quality X-ray data. *Phys. Rev. E.* **62**:4000–4007 (2000).

28. O. Hernell, J. E. Staggers, and M. C. Carey. Physicochemical behavior of dietary and biliary lipids during intestinal digestion and absorption. 2. Phase behavior and aggregation states of luminal lipids during duodenal fat digestion in health adult human beings. *Biochemistry* **29**:2041–2056 (1990).
29. M. W. Rigler and J. S. Patton. The production of liquid crystalline product phase by pancreatic lipase in the absence of bile salts. *Biochim. Biophys. Acta.* **751**:444–454 (1983).
30. G. Cevc, and D. Marsh. In "*Phospholipid bilayers, physical principles and models*", Wiley, New York, 1985, chapter 12.
31. J. Israelachvili, D. J. Mitchell, and B. W. Ninham. Theory of self-assembly of hydrocarbon amphiphiles. *J. Chem. Soc. Faraday II* **72**:1525–1568 (1976).
32. J. Israelachvili. In "*Intermolecular and Surface Forces*", 2nd Edition, Academic, New York, 1991
33. E. S. Lutton. Phase behavior of aqueous systems of monoglycerides. *J. Am. Oil Chem. Soc.* **42**:1068–1070 (1965).
34. N. Krog. Food emulsifiers and their chemical and physical properties. In S. Friberg, and K. Larsson (eds.) *Food Emulsion*, Marcel Dekker, New York, 1997, pp. 141–188.
35. J. S. Patton and M. C. Carey. Inhibition of human pancreatic lipase-colipase activity by mixed bile salt-phospholipid micelles. *Am. J. Physiol.* **241**:G328–G336 (1981).
36. C. Tanford. Theory of micelle formation in aqueous-solutions. *J. Phys. Chem.* **78**:2469–2479 (1974).
37. P. W. Westerman. Physicochemical characterization of a model digestive mixture by ^{2}H NMR. *J. Lipid Res.* **36**:2478–2492 (1995).
38. J. E. Staggers, O. Hernell, J. E. Staggers, and M. C. Carey. Physical-chemical behavior of dietary and biliary lipids during intestinal digestion and absorption. 1. Phase behavior and aggregation states of model lipid systems patterned after aqueous duodenal contents of healthy adult human beings. *Biochemistry* **29**:2028–2040 (1990).
39. D. P. Cistola, D. Atkinson, J. A. Hamilton, and D. M. Small. Phase behavior and bilayer properties of fatty acids: hydrated 1:1 acid soaps. *Biochemistry* **25**:2804–2812 (1986).
40. M. Lindstrom, H. Ljusberg-Wahren, K. Larsson, and B. Borgstrom. Aqueous lipid phases of relevance to intestinal fat digestion and absorption. *Lipids* **10**:749–754 (1981).
41. D. M. Small. A classification of biologic lipids based upon their interaction in aqueous systems. *J. Am. Oil Chem. Soc.* **45**:108–119 (1968).
42. M. Svard, P. Schurtenberger, K. Fontell, B. Jonsson, and B. Lindman. Micelles, vesicles and liquid crystals in the monoolein-sodium taurocholeate-water system. Phase behavior, NMR, self-diffusion and quasi-elastic light scattering. *J. Phys. Chem.* **92**:2261–2270 (1988).